Automation in Construction 40 (2014) 68–83

Contents lists available at ScienceDirect

Automation in Construction

journal homepage: www.elsevier.com/locate/autcon

Application of RFID tracking to the optimization of function-space assignment in buildings

Ren-Jye Dzeng [a,*], Chong-Wey Lin [b], Fan-Yi Hsiao [c]

[a] Department of Civil Engineering, National Chiao Tung University, 1001, University Road, Hsinchu, Taiwan, ROC
[b] Department of Commutation and Technology, National Chiao Tung University, Taiwan, ROC
[c] Department of Civil Engineering, National Chiao Tung University, Taiwan, ROC

ARTICLE INFO

Article history:
Accepted 28 December 2013
Available online 4 February 2014

Keywords:
RFID
Optimization
Function–space assignment
fmGA
Genetic algorithm

ABSTRACT

Function–space assignment, which allocates a function for each space in a facility, is one of the most important factors in determining the usability performance of a building. Most architects renovate a building based on their personal perception of how the occupants might use the building instead of quantitatively analyzing their use behaviors. This study developed a function–space assignment optimization model based on the occupants' movement data as tracked by RFID technology. The model mines the movement data by constructing patterns and calculating the relation values between functions. The search for the best assignment is based on the fast messy genetic algorithm (fmGA) with the objective function incorporating the preference of space size and the minimization of the distance for movement required by the occupants during the performance of their daily activities. The proposed model incorporated building-block filtering mechanism in the fmGA problem-solving process to generate enough copies of the good building blocks so more copies would remain for subsequent processing. The paper also describes two experiments that evaluate the performance of the model and compare the performances of the models with and without the building-block filtering mechanism.

1. Introduction

Function–space assignment, which allocates a function to each space in a facility, is one of the most important factors in determining the usability performance of a building. For example, in an educational building, the layout of classrooms, the administration office, laboratories, etc., affects how occupants move and the distances required to fulfill their activities in the facility. Kalay [1] noted that function assignment only works in very limited areas of architectural design, primarily due to the lack of quantifiable data. Instead of relying on the facility administrator's trial and error to find the optimum layout, mathematic optimization algorithms that have been applied in the layout of hospitals, factory assembly lines, and construction sites become feasible once quantifiable data about occupants' movements are available.

To collect quantitative data about occupants' movement, instead of relying on subjective experience or opinions, one may actually monitor the occupants' movement manually or by using currently available monitoring technologies, such as surveillance cameras and positioning technologies via radio frequency identification (RFID), wireless fidelity (Wi-Fi), etc. These positioning technologies have become more accurate and affordable in recent years and also have a variety of applications, as reviewed in the following section.

When quantitative data about occupants' movement behaviors are available, the layout may be optimized for certain specific objectives, such as the minimization of movement distances or preferred space size. In architecture, optimization techniques have been used primarily for solving problems of site layout, facility layout, structural design, and building performance [2–5]. Facility layout optimization involves finding feasible topology and the dimensions of interrelated objects that meet all of the design requirements and maximizing design preferences [6]. Previous research has developed several formulations for the optimization of facility layout problem. For discrete formulations, the quadratic assignment problem (QAP) [7] is the most commonly encountered in the literature.

The QAP is one of the most difficult problems in the NP-hard class. Exact approaches are generally unable to solve problems of size larger than $n = 15$ [9]. Because exact solutions require large expenditures of time and money, it may not be worthwhile to search for the optimum solutions except in rare circumstances [10]. For this reason, several heuristics and meta-heuristics approaches have been developed to search sub-optimal solutions within a reasonable time limit.

There are two types of heuristic approaches, construction methods and improvement methods. Construction methods generate sub-optimal permutations from scratch by assigning functions to spaces one by one based on prioritized criteria. Examples are CORELAP [11], ALDEP [12], COFAD [13] and SHAPE [14]. Instead of starting from scratch, improvement methods begin with a feasible solution and try to systematically improve it by searching for other nearby solutions.

* Corresponding author. Tel.: +886 916005996.
E-mail addresses: rjdzeng@mail.nctu.edu.tw (R.-J. Dzeng), cwlin@mail.nctu.edu.tw (C.-W. Lin), minlove.xiao@gmail.com (F.-Y. Hsiao).

0926-5805/$ – see front matter © 2014 Elsevier B.V. All rights reserved.
http://dx.doi.org/10.1016/j.autcon.2013.12.011

The process is continued until no improvement can be found. Examples of this method are CRAFT [15], FRAT [16] and DISCON [17].

Before the end of the 1980s, most of the proposed heuristic approaches for combinatorial optimization problems were specific and dedicated to a given problem. Since that time, this paradigm has changed. More general methods have appeared, known as meta-heuristics [18]. Several of these methods are based on some type of simulation of a natural process studied within another field of knowledge. Recently, numerous researchers have developed meta-heuristics approaches for the QAP. Solimanpur [19] developed an ant algorithm for a sequence-dependent single row machine layout problem. Yeh [8] adopted annealed neural networks and Hopfield neural networks to solve preferences in a hospital building layout problem. Liang [20] developed the multi-searching technique of tabu algorithms to improve facilities layout performance through several previous examples, including a pre-cast yard, construction site and hospital. Cheung [21] developed the swap method of simple genetic algorithms to determine the least cost arrangement for a pre-cast yard layout. Jang [22] also employed simple genetic algorithms to optimize the layout of multi-floor construction material.

The simple genetic algorithm (sGA) is one of the meta-heuristic approaches. First developed by Holland [23] in 1975, sGA is an efficient and commonly used algorithm [21,22,24,25]. Goldberg et al. [26] subsequently developed the messy genetic algorithm (mGA) in 1989 to improve the sGA. Several experiments have proven that the mGA is much better at solving permutation problems than the sGA. In 1993, Goldberg [27] developed the fast messy genetic algorithm (fmGA) to reduce the high memory consumption of operation processes. Over the years, mGA and fmGA have been used successfully in water distribution system design [28], the dispatching of ready mixed concrete trucks [29], the design of fuzzy control systems [30], solutions for clustering problems [31], and learning classifier systems [32–35]. Because of its advantages, we used fmGA to search for the optimal solution in this research.

The presented research aims to optimize function–space assignment by sensing the occupants' movement data. The proposed model first tracks occupants' movements in a multi-floor building and then develops a systematic method which can analyze these movement data and optimize function assignment for the building. In addition, the fmGA is employed to find the best assignment or improve the assignment according to the desired objectives, such as preferred space size and minimized movement distance. Finally, an experiment with a real case was conducted to evaluate the performance of the proposed model.

2. Location tracking technology

With the increasing use of location-based services (LBS) in mobile communication, GPS appears to be the most popular solution for outdoor location systems. However, for indoor location applications, other technologies are more common than GPS because of the limitation caused by indoor barriers that block satellite signals. Examples of other technologies for indoor applications are Wi-Fi based systems [36], infrared systems [37], ultrasound [38], scene analysis [39], and radio frequency identification [40].

Based on Tesoriero et al. [41] and Li and Becerik-Gerber [40], the following section summarizes the strengths and weaknesses of these technologies. The Wi-Fi-based system uses existing IEEE 802.11 infrastructure and shows advantages in the cost of deployment. However, the performance of the Wi-Fi based system decreases in multi-floor or densely partitioned indoor environments because the signal reflections and dynamic network conditions may affect signal readings. The infrared system has the advantages of low power consumption, low cost and compact size. Nevertheless, the infrared system is sensitive to sunlight so it is not suitable for non-enclosed spaces. Ultrasound technology is inexpensive, easy to install, and suitable for precise measurements. However, the installation and maintenance costs are comparatively high because of the requirement for dense deployment. The scene analysis technique analyzes images of multi-cameras that monitor target areas and is precise at room level but is high cost. RFID technology has the advantages of durability, rich data capacity, repetitive read/write capabilities, and non-contact features [40,42]. However, active RFID tags usually require periodic battery replacement for approximately every 5–10 years [43].

Our research required a location technology that is able to track occupants' movement between multiple partitioned indoor spaces in a multi-floor building using corridors that can be exposed to sunlight. Thus, the Wi-Fi, infrared, ultrasound, and scene analysis technologies are not suitable. As Lionel et al. noted [44], the active RFID system for indoor location sensing is a viable and economical option; therefore, we chose RFID for our location technology.

RFID technology is a wireless sensor technology based on electromagnetic signal detection [45]. As shown in Fig. 1, a typical RFID system consists of two main components, a reader and a tag, and operates at a certain frequency. The tag, containing a microchip and an internal antenna, is attached to the object to be tracked. Each tag, with a unique ID, can store the object-related data, and send the data to a reader upon its request. A reader, containing a transceiver and an external antenna, reads/writes data from/to a tag via radio frequency and transfers data to a host computer for later retrieval and analysis.

While RFID technology has already seen significant beneficial applications in manufacturing, retail, transport and logistics industries over the years, its potential applications in the construction industry have only begun to be explored. However, RFID technology is not completely new to the construction industry. Jaselskis et al. [46] envisaged its possible applications in construction, including concrete processing and handling, cost coding for labor and equipment, and materials control. Recently, more RFID-related applications in the construction industry have become available. For example, by combining radio and ultrasound signals, Jang and Skibniewski [47] developed an embedded system for tracking construction materials and equipment. Goodrum et al. [48] explored the applications of RFID for tool tracking on construction job sites. Dziadak et al. [49] developed a model for the 3D location of buried assets based on RFID technology. Domdouzis et al. [50] explored the applications of RFID in the construction industry for the automated tracking of pipe spools and valued items and in an on-site inspection support system. Tzeng et al. [51] explored the verification tests of interior decorating materials combining RFID system recognition. Wang [52] explored how to improve construction quality inspection and management via RFID technology. To assist logistics and progress management, Chin et al. [53] combined RFID with 4D CAD to develop an information system. Yin et al. [54] developed a pre-cast production management system utilizing RFID technology. Li et al. [55] proposed an RFID-based location-sensing algorithm to perform a study on evaluation of indoor location sensing using RFID tags. In summary, all of the related research has tracked objects, and none have focused on the tracking of human movement to facilitate the functional layout of a building.

3. Research problem

Taking a real renovation project of an educational facility as an example, an existing public building with multi-floors requires renovation, and the owner and the architect plan to adjust the functions of the spaces in the building during renovation based on their usage experience in order to accommodate the usability problems. The function provided by a space is fixed once the function–space assignment is finalized. There are several types of occupants, and they move around the spaces in the building based on the activities which they have been formally assigned or in which they are personally interested. Some activities occur periodically and some do not. Some activities require an occupant to participate at specific times, and some allow them to participate at will and at their preferred times. Each occupant has an identification object so that their individual movement can be detected. The objective of the adjustment of space functionality is to minimize the

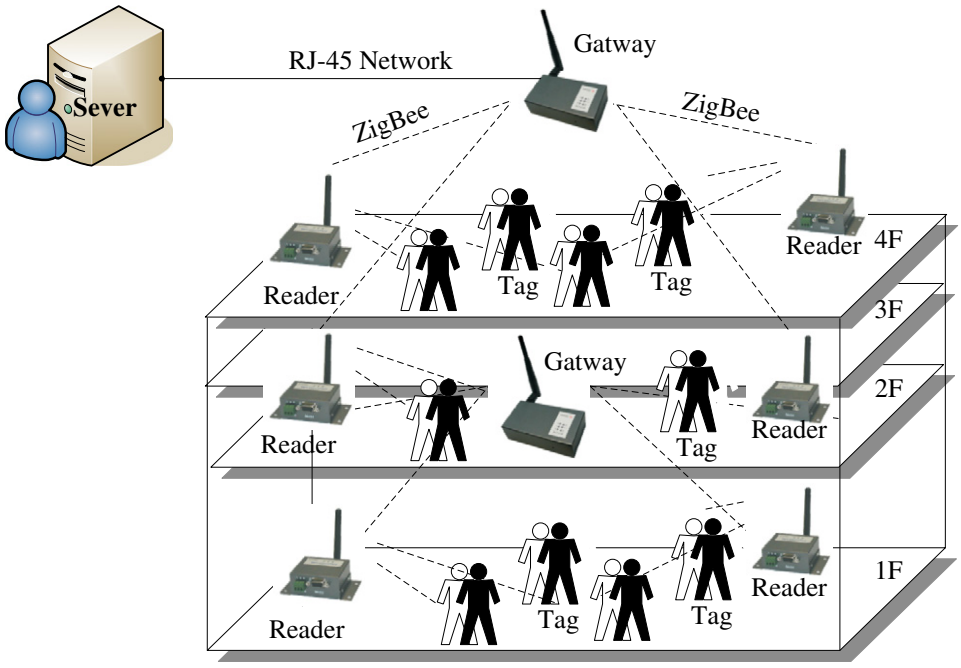

Fig. 1. Tracking occupants' movement by the RFID technology.

total occupants' movement distance and to find the best assignment based on preferred space size.

4. The proposed model

The proposed model consists of 3 modules, namely movement tracking and positioning, occupants' movement analysis, and optimization as illustrated in Fig. 2. The three modules are described as follows.

4.1. Movement tracking and positioning

For tracking the occupants' movements, we used an active RFID positioning approach, and the movement tracking devices included readers, tags, and gateways. As shown in Figs. 1 and 2, a reader was installed at each tracked space, and occupants carrying RFID-tagged ID cards were detected once they moved in and out of the space. The gateway was responsible for acquiring the terminal data from the readers. The number of required gateways, usually operating at 2.4 GHz, depended on the accessibility of the wireless signals. Based on our field test, we followed certain guidelines to determine the installation location of each reader. A reader was installed in each space we intended to monitor. We determined that the most suitable place to install a reader was far from neighboring aisles and close to open windows on the same side as the associated gateway. Placing the reader far from neighboring aisles reduced the RSSI reading of tags merely passing through those aisles, allowing us to distinguish them from the tags that actually entered the monitored space.

The manufacturer's proprietary algorithm was used for detecting the RSSI of each tag to determine each tag's position. As shown in Fig. 3, tags were detected by readers installed at various positions, and readers were configured to send tag position data to the server, through the gateways, every 5 s. Because a tag could be detected by multiple readers, each tag's associated reader was identified according to the reader that had the highest RSSI for that tag; the tag was then assumed

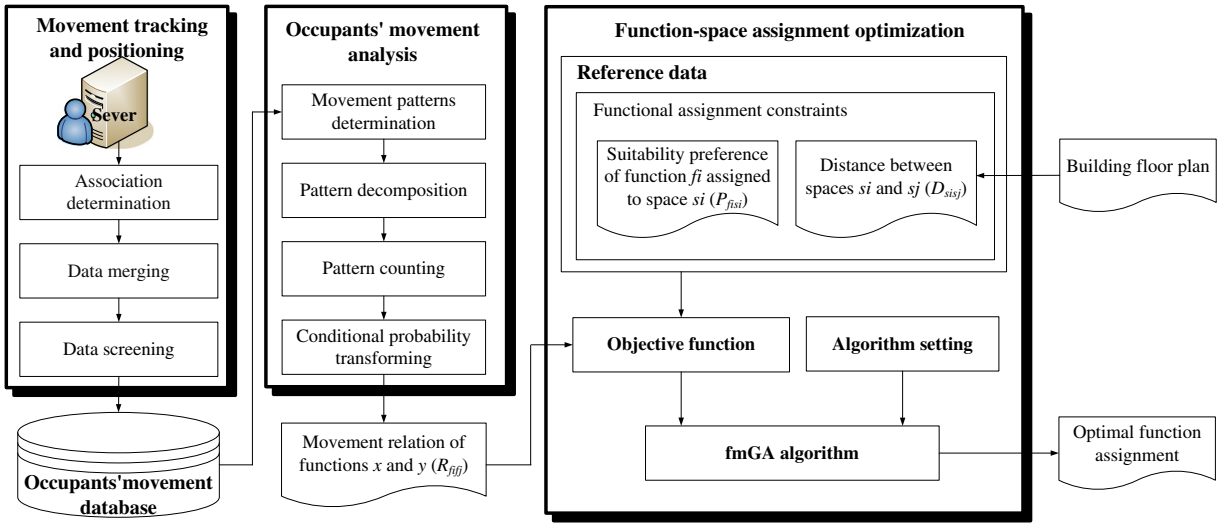

Fig. 2. Function–space assignment.

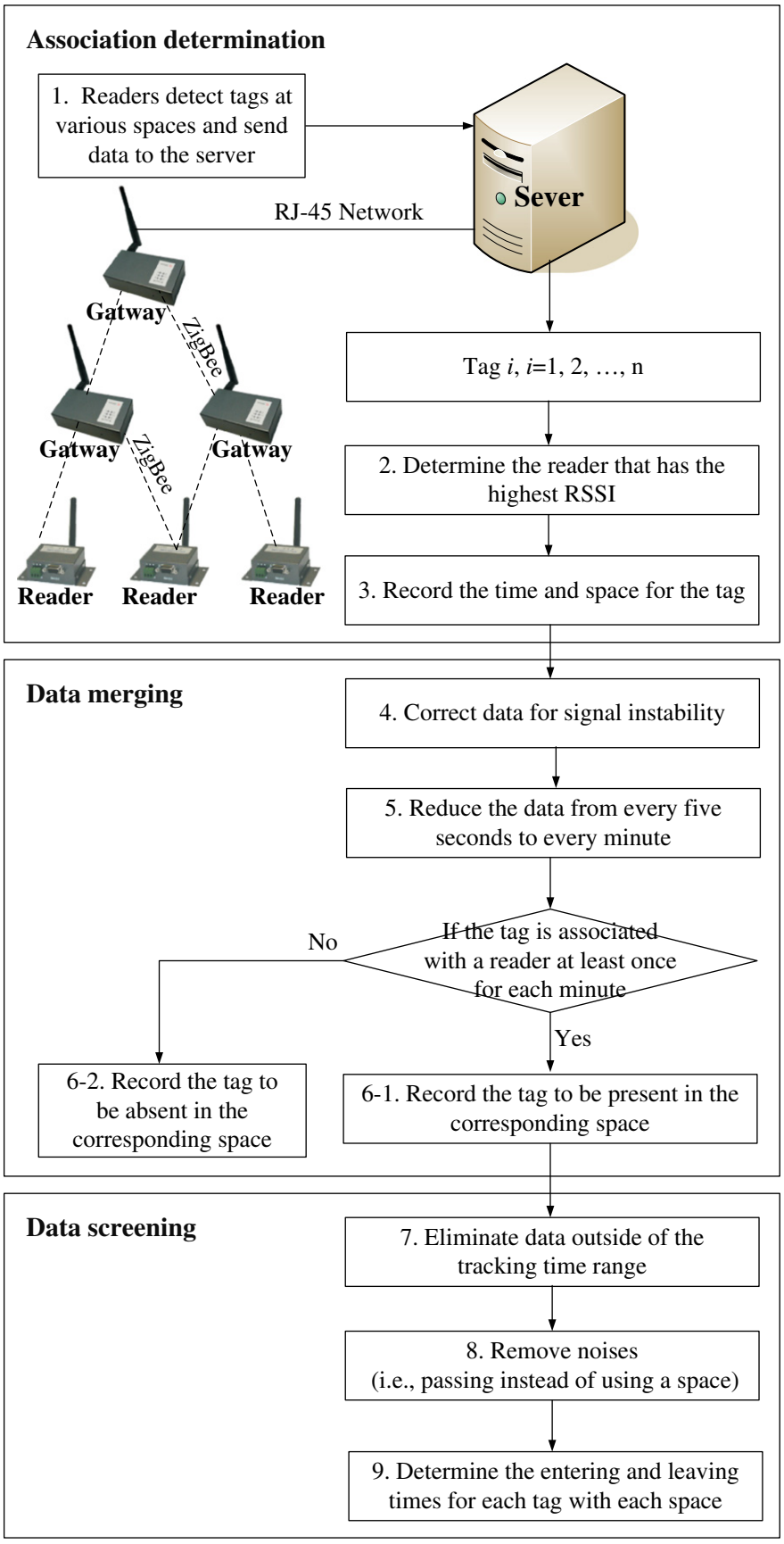

Fig. 3. Spatial location tracking of each tag using RSSI.

to be in that reader's space at the detected time. The server collected data on the tag and its associated space at 5-second intervals. Our purpose was to determine whether a tag was inside a particular space. We did not need to estimate the precise location of the tag according to the RSSI strengths from the three readers.

In the data merging, to accommodate the instability of signal, the tag would be determined to be present in the corresponding space during a particular minute if the tag was associated with a reader at least once during that minute (i.e., 1 out of 12 times). In the data screening, the server eliminated data outside of the tracking time range and only kept the data obtained within 8:00 AM and 10:00 PM on weekdays. And the data was furthered merged to determine the entering and leaving times of a tag for the associated space according to the *minimum stay time* specified by the user. In this step, the server removed noisy data such as in the situations where an occupant entered a space and left from it right away, or an occupant stood outside of but adjacent to a space instead of being actually inside the space. The *minimum stay time* required to be considered as using the space was set to 1 min for the library and administration office and 5 min for the rest of the functions. Thus, a tagged student who entered the administration office to retrieve mail and left after 2 min was considered to have used the office once. A student who entered a classroom to collect some textbooks he forgot during a previous lecture and left the classroom after 2 min was not considered to have used the classroom.

4.2. Occupants' movement analysis

The analysis of occupants' movement involves four steps, i.e., movement pattern determination, pattern decomposition, pattern counting, and conditional probability transforming, as shown in Fig. 4. Movement pattern determination data mined an occupant's movement pattern between spaces on each day. One can set up a threshold of *maximum break time* for a movement between two spaces to be considered as part of a pattern. For example, one may set the *maximum break time* to be 30 min. Thus, if the time interval of the detections of a tag at two different spaces is smaller than 30 min, the corresponding occupant's movement between the two spaces will be considered as a movement pattern; otherwise, the uses of two spaces will be considered as independent usages.

Pattern decomposition breaks down the daily movement pattern of an occupant into pairs of spaces for later counting purposes. For example, as shown in the movement pattern table in Fig. 3, Tag 120 has used space *a*, *a*, *b*, *c*, *c*, and *d* on March 1st of 2011. The breakdown results in pairs of *aa*, *ab*, *bc*, *cc*, and *cd*.

Pattern counting counts the occurrence of each pair of spaces in the breakdown result of the previous step in preparation for constructing the interactive preference table. As shown in the pattern counting table of Fig. 3, each number represents the number of occurrences of the corresponding pair (from a column space to a row space). For example, the use pattern *aa* (the use of space *a* following space *a*) occurs 4 times, *ab* occurs 1 time, and so on.

The fourth step is to calculate the conditional probability of a row space given a column space, as shown in the movement relation table of Fig. 4. For example, the likelihood of using spaces *b*, *c*, *and d* after using space *c* is 1/5 (0.2), 3/5 (0.6), and 1/5 (0.2), respectively.

4.3. Function–space assignment

The optimization module maximizes the objective function under defined constraints by finding the best assignment of functions to spaces. The objective function used in this research was based on the concept proposed by Koopmans and Beckman [7], which was previously applied by Jo and Gero [56] in assigning functions to spaces of equal size in an office building. Yeh [8] modified the objective function to enable the assignment of functions to spaces with different sizes in a hospital. We used the objective function proposed by Yeh [8] but with two primary differences. First, the objective function of this research was based on the interactive preference derived from the tracking of real occupants' movements instead of subjective judgments. Secondly, while Yeh [8] optimized the objective function using an annealed neural network, this research used a newly developed algorithm called the fast messy genetic algorithm.

Eq. (1) is the objective function, which is a weighted average of two parts. First, $(X_{fisi} \times P_{fisi})$ represents the assessment of the suitability of a function assigned to a space. For example, a classroom assigned to a large space is more suitable than to a small space. Secondly, $(X_{fisi} \times X_{fjsj} \times D_{sisj} \times R_{fifj})$ represents the assessment of a function assigned to a space from the perspective of the moving distance $(X_{fisi} \times D_{sisj})$ based on the movement relation $(X_{fjsj} \times R_{fifj})$. For example, strong related functions assigned to neighboring spaces may have a higher assessment value than that to spaces at a distance. Table 1 is an example of $X_{f_i s_i}$, where 5 functions (f_1 to f_5) are to be assigned to 5 spaces (s_1 to s_5). $X_{f_i s_i}$ indicates that f_1 is assigned to s_1, f_2 to s_3, f_3 to s_2, f_4 to s_5, and f_5 to s_4.

$$\text{Max } O = W_1\left(\frac{\sum_{f_i}\sum_{s_i} X_{f_i s_i} \times P_{f_i s_i}}{n}\right) + W_2\left(\frac{\sum_{f_i}\sum_{s_i}\sum_{f_j}\sum_{s_j} X_{f_i s_i} \times X_{f_j s_j} \times D_{s_i s_j} \times R_{f_i f_j}}{n}\right) \quad (1)$$

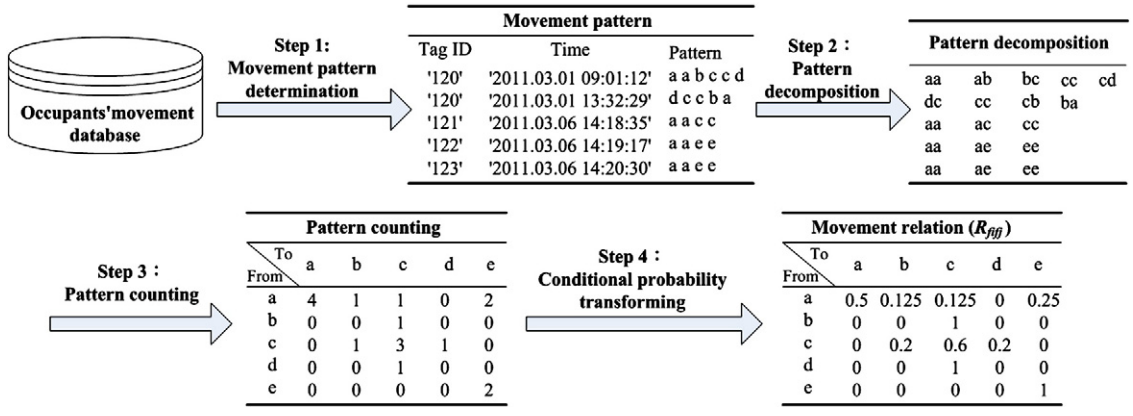

Fig. 4. Occupants' movement analysis.

Table 1
Permutation matrix with five functions.

$X_{f_i s_i}$		Space				
		s_1	s_2	s_3	s_4	s_5
Function	f_1	**1**	0	0	0	0
	f_2	0	0	**1**	0	0
	f_3	0	**1**	0	0	0
	f_4	0	0	0	0	**1**
	f_5	0	0	0	**1**	0

Subjected to

$X_{f_j s_i} = 0$ if $X_{f_i s_i} = 1$ and $f_j \neq f_i$,
$X_{f_i s_j} = 0$ if $X_{f_i s_i} = 1$ and $s_j \neq s_i$.

where O: objective function;

$X_{f_i s_i}$: permutation matrix variable (i.e., the value is 1 if function f_i is assigned to space s_i, and is 0 if not assigned to s_i);
$P_{f_i s_i}$: suitability preference of function f_i assigned to space s_i (e.g., the library function prefers large spaces, the value for the library function assigned to large, medium, and small spaces were 1, 0, and 0, respectively.);
$D_{s_i s_j}$: distance between spaces s_i and s_j;
$R_{f_i f_j}$: movement relation of functions f_i and f_j (i.e., the value is between 0 and 1, where 0 represents no sequential movement pattern exists between functions f_i and f_j, and 1 represents the use of f_i always followed by the use of f_j);
n: total number of functions;
$W1$: the assessment weight of the suitability of a function assigned to a space (the weight between 0 and 1).
$W2$: the assessment of a function assigned to a space from the perspective of the moving distance (the weight between 0 and 1).

5. fmGA for function assignment optimization

The fmGA can efficiently find optimal solutions for large-scale permutation problems. There are three distinct features that differentiate the fmGA from the sGA [29,35]: (1) chromosomes of variable length can be adopted in fmGA; (2) the optimization process contains both a primordial and a juxtapositional stage; and (3) competitive templates are adopted to retain the most outstanding gene building blocks in each generation. Because of the large number of functions and spaces usually involved in a building, the fmGA representation was used.

5.1. Problem-solving process

The function–space assignment is optimized using fmGA using the process flow shown in Fig. 5. The required input data include the suitability preference of function f_i assigned to space s_i (P_{fisi}), distance between spaces s_i and s_j (D_{sisj}), the movement relation of functions f_i and f_j (R_{fifj}), and fmGA parameters. The process consists of 4 primary steps described as follows.

5.1.1. Step 1 Randomly generate a competitive template

The first step is to randomly generate a competitive template, which is a problem-specific, fixed-bit string that is randomly generated or found during the search process [27]. The competitive template is used to make up for the missing genes in the latter process when chromosomes are under-specified.

The fmGA process consists of inner and outer loops. Each inner loop is called an era and each outer loop is called an epoch. Thus, the execution of the maximum number of eras defined by era_max completes an epoch. The execution of the maximum number of epochs defined by epoch_max terminates the fmGA evolution process.

The inner loop consists of three phases [27]: (1) the initialization phase—a population with sufficient chromosomes is created to contain all possible building blocks (BBs) of the order k, where BBs refer to partial solutions of a problem; (2) the primordial phase—bad genes are filtered out to maintain only the chromosomes with good fitness; and (3) the juxtaposition phase—those good alleles (BBs) are rebuilt by cut-splice and mutation operations to form a high quality generation, which tends to generate an optimal solution.

5.1.2. Step 2 Initialization phase

To ensure a sufficient quantity of chromosomes, the population size of each era is determined by Eq. (2), as suggested by Goldberg [27]. In addition, n chromosomes are randomly generated in this phase, so the fitness of each chromosome is evaluated based on the objective function, defined by Eq. (1).

$$n = \frac{\binom{l}{\lambda}}{\binom{l-k}{\lambda-k}} 2c(\alpha)\beta^2(m-1)2^k \tag{2}$$

where

l: the problem length;
k: the order of BBs;
λ: a random value, generally set to be $l - k$, $k<\lambda \leq l$;
$c(\alpha)$: the square of a normal random deviate corresponding to a tail-probability α;
β: the signal-to-noise ratio which is the ratio of the fitness deviation to the difference between two competing BBs (i.e., the ratio of a chromosome with the optimum fitness (O) to those with the second best fitness (O')in the same era, $\beta = O/O'$);
m: BBs coefficient.

5.1.3. Step 3 Primordial phase

There are two operations in the primordial phase, namely building-block filtering and threshold selection. Building-block filtering includes building-block selection and random gene deletion. The key to building-block filtering is to pump up enough copies of the good building blocks so that even after random deletion eliminates a number of copies, there remain one or more copies for subsequent processing [57].

According to Goldberg et al. [58], having enough good building blocks provides more good chromosomes for subsequent processing. Thus, they used a generic threshold mechanism, where the selection between two strings was only permitted if they shared a greater than expected number of genes in common, which restricts the competition between building blocks with little in common. However, the threshold was not needed in our case because all of the chromosomes share the same set of genes (i.e., the same set of functions are assigned to a set of genes).

5.1.4. Step 4 Juxtaposition phase

The purpose of the juxtaposition phase is to change chromosomes, and it includes the cut-splice and mutation operations. The cut-splice operator, similar to the crossover operator in the sGA, is used to recombine different strings to create new strings [29]. At first the cut-splice operation is applied to a predetermined probability (i.e., cut and splice probability P_c, P_s) of the chromosomes. After performing the cut-splice operation, the fitness value of a chromosome may be higher or lower than (or equal to) that of the competitive template in the previous era. The mutation is applied to a predetermined probability (i.e., mutation rate P_m) of the chromosomes with lower (or equal) fitness values because they are less competitive solutions and vice versa.

The newly generated and existing chromosomes are stored in a pool, representing the population of the era. The best chromosome with the highest fitness value will be selected and replaces the competitive template if its fitness is higher. In addition, a predetermined proportion of

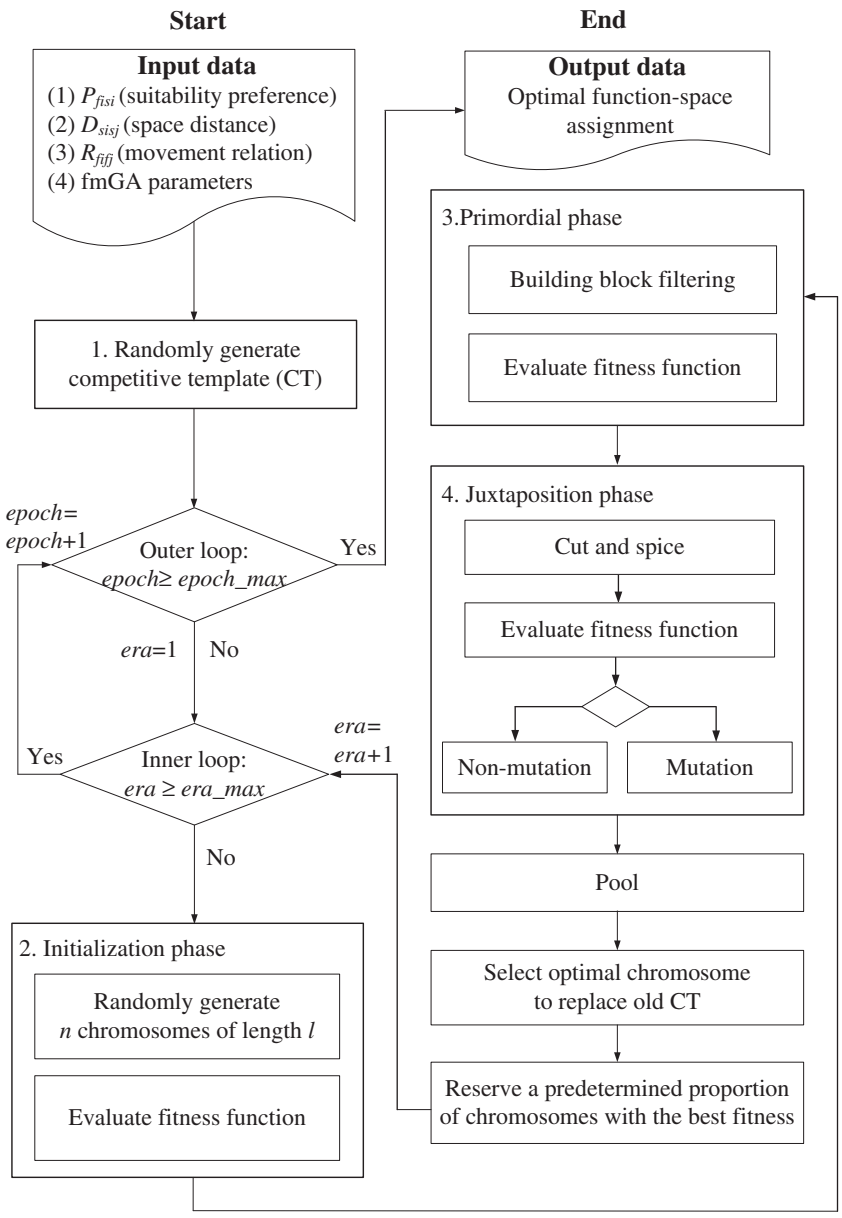

Fig. 5. Problem-solving process for function–space assignment optimization.

the best population is kept and carried to the next era. Steps 2 to 4 are iterated for a predetermined number of times, which completes an epoch. Such a process is iterated until the fitness value of the best chromosome converges or the predetermined maximum number of epochs is reached.

5.2. Problems with over-/under-specifications

In the fmGA, a chromosome is composed of two pairs of genes, i.e., an allele locus and an allele value. Fig. 6 shows a chromosome example C_0, in which each allele locus represents a space while an allele value represents a function assigned to the corresponding space. The length

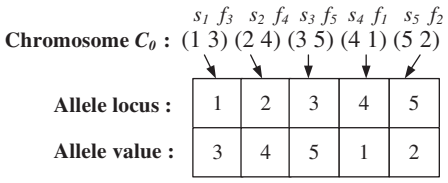

Fig. 6. Messy chromosome.

of the chromosome determines the number of spaces to which functions are assigned. Thus, the example represents a problem of assigning five functions to five spaces, e.g., functions f_3 to space s_1 and f_4 to s_2.

Because the messy chromosomes may have various lengths after the cut-splice process, they may be "over-specified" or "under-specified". Fig. 7 shows an example that illustrates this problem. Before the cut, both chromosomes C_1 and C_2 are valid strings, where each space is assigned to a unique function. After cutting and splicing, the two chromosomes switch the genes on the right-hand side of the randomly selected cut point. The switch results in over-specified chromosomes, e.g., space s_2 is assigned to functions f_3 and f_4 in C_1', and s_4 is assigned to f_2 and f_4 in C_2'. It also results in under-specified chromosomes, e.g., no functions are assigned to s_4 in C_1' and s_1 in C_2'.

The use of an integer in this research instead of a binary value for genes complicates the over- and under-specified problems. Fig. 8 shows the proposed process to solve the over- and under-specified problems existing in C_1'. To fix the over-specified chromosome, the string is scanned from left to right with the first-come first-serve rule. In Step 1, genes (*2 4*) and (*1 5*) are removed from C_1' because functions for spaces s_1 and s_2 are already assigned in genes (*1 2*) and (*2 3*). Step 2

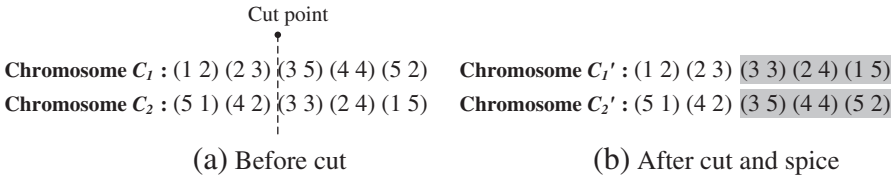

Fig. 7. Cut-splice process.

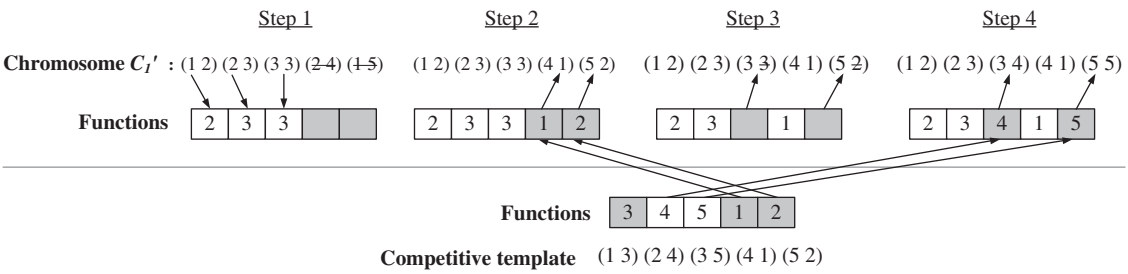

Fig. 8. Evaluation of over-specified and under-specified chromosomes.

fills the removed genes with the genes at the corresponding spaces in the competitive template. However, although C_1' now has all of its spaces specified, the filling results in over- and under-specified functions. Step 3 removes the functions of genes (*3 3*) and (*5 2*) because functions 3 and 2 have already been assigned to space s_2 and s_1. Step 4 filters out the genes with functions already specified in C_1' (i.e., (*1 3*), (*4 1*), and (*5 2*)) after the removal, assigns the leftover functions to the unspecified spaces in C_1' from left to right.

6. Case and experiment

We conducted an experiment based on a real case to prove the research concept and to evaluate the performance of the proposed system. The following sections first give a case overview, the RFID field test, the variables of function–space assignment, and then present the result of function–space assignment, followed by the comparison of fmGA performance with and without building-block selection.

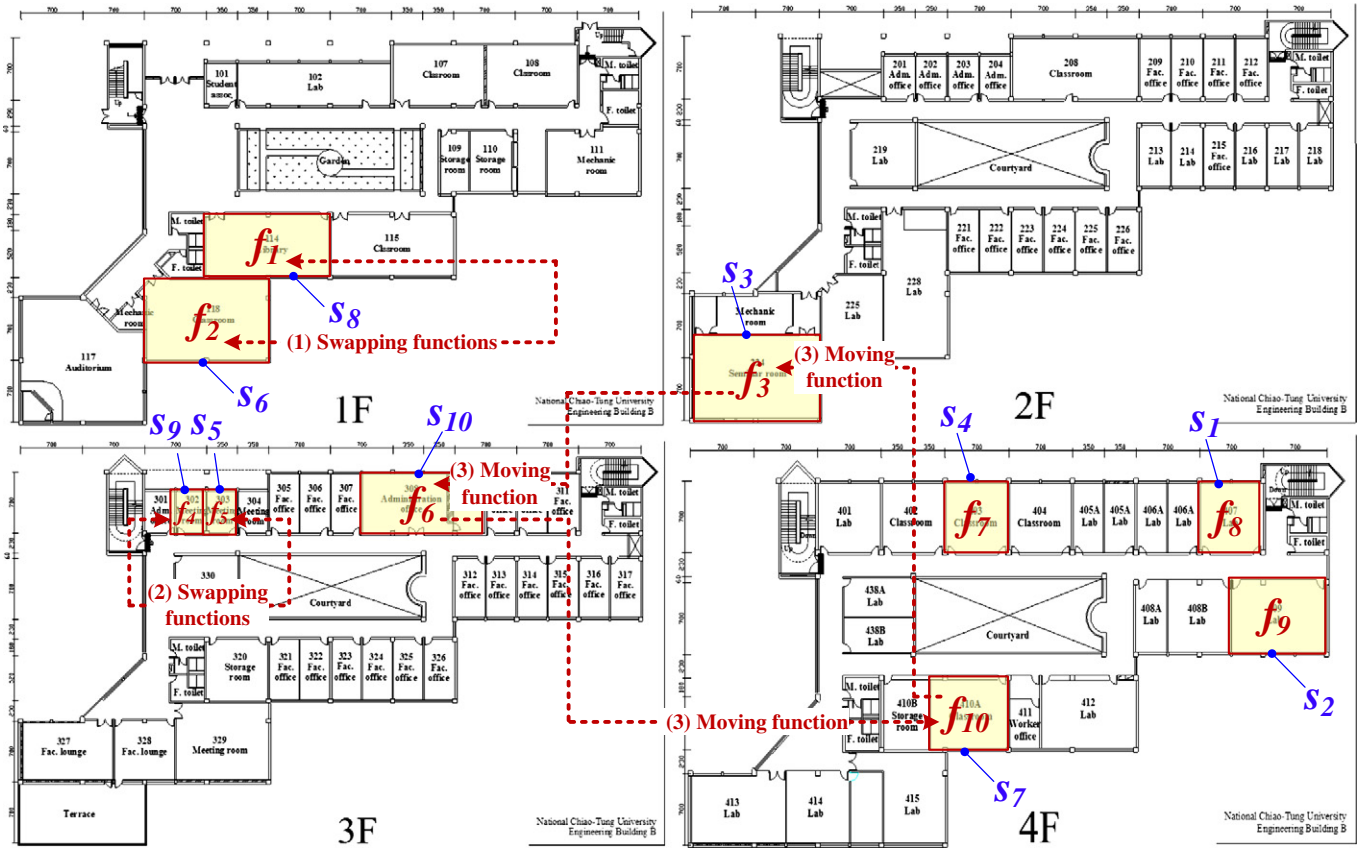

Fig. 9. Comparison of architect's function assignment and the assignment result R_1 (objective value = 1.10471 vs. objective value = 1.26821).

6.1. Case

The case used in this experiment is the building of the Civil Engineering Department of National Chiao Tung University in Hsinchu, Taiwan. The building is a 4-story courtyard building with a total floor area of 6616 m^2, as shown in Fig. 9. There are 3 main entrances on the ground floor and two staircases. The spaces of the building include a garden, a library, an auditorium, an administration office, classrooms, laboratories, meeting rooms, seminar rooms, faculty offices, mechanical rooms, and storage rooms. The building was renovated by an architect in 2010.

Limited by the availability of RFID readers, we only tracked 10 key spaces (numbered from s_1 to s_{10}), consisting of an administration office, a library, a seminar room, 2 laboratories, 2 meeting rooms, and 3 classrooms, which were situated separately on the 4 floors of the building. There were 98 students (23% of the total number of college and graduate students) participating in this experiment. Each of them carried a Helicomm IP-Link 5110 active RFID tag while performing their daily activities in the building for 8 weeks during the middle and end of a semester in 2011. Although the movement was tracked 24 h a day during the experiment period, only the data obtained within 8:00 AM and 10:00 PM on weekdays (Monday to Friday) were used. The 10 tracked spaces were equipped with Helicomm IP-Link 2220 readers, and the data were transmitted wirelessly through two IP-Link 2220E gateways. The collected data were sent to another gateway, connected to the intranet network through RJ-45, to a computer server. The wireless network operated on a 2.4-GHz global ISM (Industrial Scientific Medical) band. The maximum transmit range is 100 m for the tag, 400 m for the reader, and 1200 m for the gateway. In addition, the maximum data rate is 250 kbps for the reader, tag, and gateway.

6.2. Field test for RFID devices

To evaluate about the spatial location tracking of each tag proposed in this research, we conducted a field test to assess the data collection accuracy of this RFID device layout. The field test consisted of two experiments. Field Test I tested the ability of the readers to detect tags in spaces under various obstructive conditions. Field Test II tested the ability of the readers to detect tags carried by participants in different ways, some of whom also carried various amounts of metal. As shown in Fig. 10, the field test devices contained 50 tags, 10 readers, 3 gateways, and 1 server. The experimental results are shown as follows.

6.2.1. Field Test I

The location of the readers is crucial to ensuring the signal transmission accuracy of active RFID devices. In active RFID, wireless communication is used to collect data; signal transmission accuracy is therefore easily affected by various obstructive conditions. The field test was designed to test the performance of the readers in spaces obstructed by various obstacles, including walls, crowds, and chalk dust. Table 2 presents the spaces under various obstructive conditions where the 10 readers were placed. Reader 4 was placed in space s_4, where it was obstructed by crowds; Reader 6 was placed in space s_6, where it was obstructed by walls, crowds, and chalk dust; Reader 7 was placed in space s_7, where it was obstructed by chalk dust; and Reader 9 was placed in space s_9, where it was obstructed by walls. The remaining readers (1, 2, 3, 5, 8, and 10) were located in unobstructed spaces s_1, s_2, s_3, s_5, s_8, and s_{10}, respectively. Each of the 50 participants in Field Test I carried a handheld tag and entered each of the 10 spaces

Fig. 10. RFID devices.

Table 2
Results of Field Test I for readers in spaces under various obstructive conditions.

Reader no.	Installationspace	Obstruction			Mean read rate (%)	Variance of read rate (%)
		Walls	Crowd	Chalk dust		
1	s_1				99.9	0.18
2	s_2				100.0	0.00
3	s_3				99.9	0.18
4	s_4		●		99.6	0.41
5	s_5				100.0	0.00
6	s_6	●	●	●	97.1	0.63
7	s_7			●	100.0	0.00
8	s_8				100.0	0.00
9	s_9	●			97.5	0.91
10	s_{10}				100.0	0.00

sequentially (Fig. 11, s_1 to s_{10}), remaining in each space for 5 min, 3 times total. In addition, the space of each reader had an antenna fixed in the appropriate direction during the field test.

Table 2 presents the field test results for the readers in spaces under various obstructive conditions. Readers 1, 2, 3, 5, 8, and 10, which were located in unobstructed spaces, exhibited read rates of up to 99.9%.

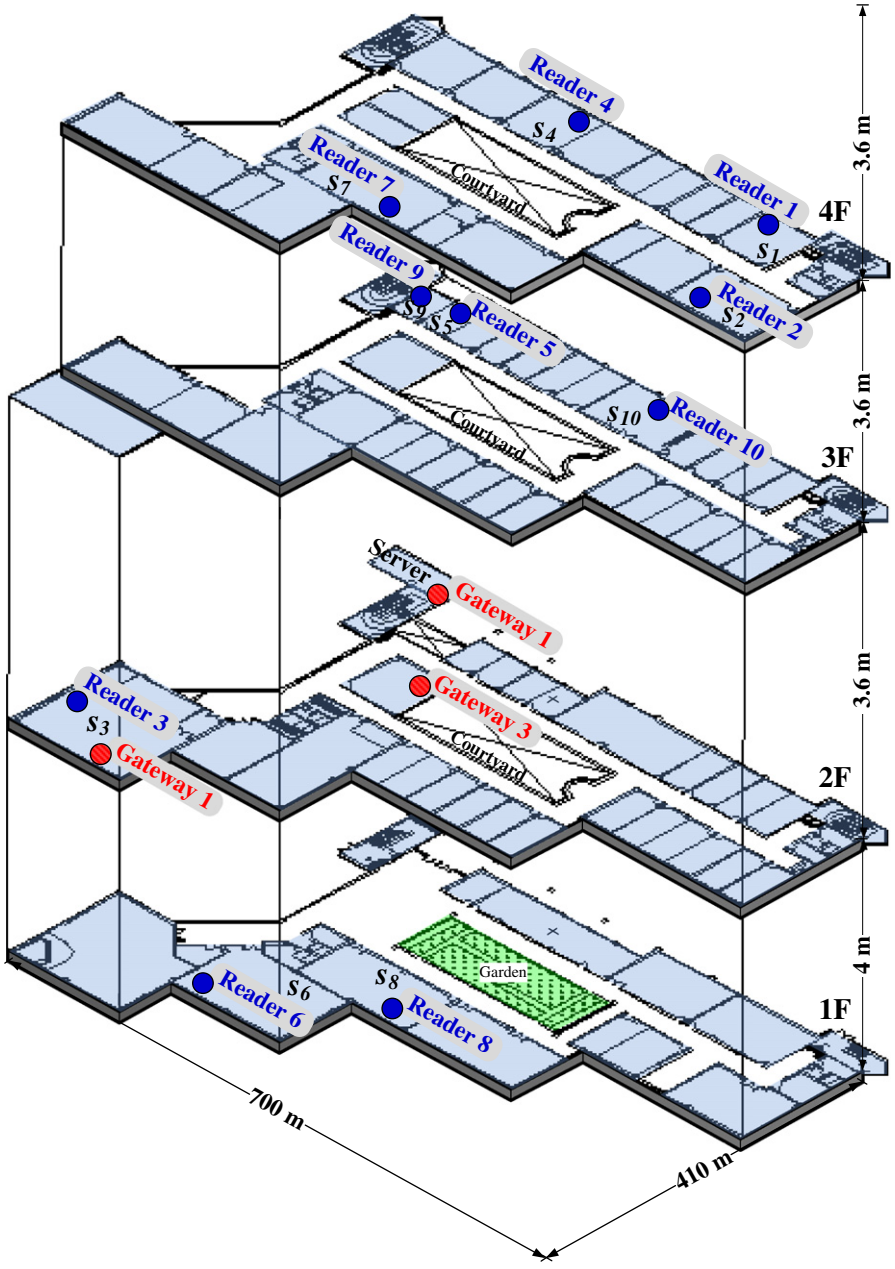

Fig. 11. Devices layout of gateways and readers.

Table 3
Results of Field Test ΠI for tag-carrying types with various amounts of metal.

Tag-carrying types		Types	Metal effect	Mean read rate (%)	Variance of read rate (%)
Naked	Holding in hand	*A*	No	100.0	0.0
		B	Low	100.0	0.0
	Hanging around neck	*C*	No	100.0	0.0
		D	Low	99.3	0.3
Enclosed	Front pocket	*E*	No	98.7	0.3
		F	Low	98.7	0.3
	Back pocket	*G*	No	98.7	0.3
		H	Low	98.0	1.0
	Backpack	*I*	No	98.0	0.0
		J	Low	97.3	0.3
		K	Middle	92.7	2.3
		L	High	67.3	1.3

Readers 6 and 9 exhibited approximately 2% ~ 3% lower read rates than the readers in unobstructed spaces did. Readers 6 and 9 were located in spaces partially blocked by walls, which affected the signal transmission between the gateways and these readers. The read rate of Reader 4 was approximately 0.3% lower than that of readers in unobstructed conditions. Readers 4 and 6 were both located in crowded spaces (Reader 4 was placed in a medium-sized classroom surrounded by other classrooms; Reader 6 was placed in a large classroom near a large auditorium). Compared with readers in unobstructed spaces, Reader 7 was placed in a space where it was obstructed by chalk dust, and its read rate was not apparently affected.

6.2.2. Field Test ΠI

Field Test II was conducted to determine the ability of readers to detect tags carried by participants in different ways, some of whom carried various amounts of metal; the results of this test are presented in Table 3. The participants carried the active RFID tags in two ways: "naked" and "enclosed." The naked tags were either held in the participant's hand or hung around the neck; the enclosed tags were placed in the participant's front pocket, back pocket, or backpack. To measure the effect of metal, certain participants who carried tags also carried various amounts of metal objects, such as keys. Certain participants carrying tags in pockets or backpacks carried low amounts of metal (i.e., two bunches of keys), whereas only participants with backpacks carried middle amounts of metal (i.e., 14-inch laptop) and high amounts of metal (i.e., 2.5-kg dumbbells). To control for the effect of metal, some participants did not carry any metal objects. The tags (naked or enclosed) and amounts of metal carried by each of the 50 participants in Field Test II are listed in Table 3. The participants walked into the 10 spaces sequentially (Fig. 11, s_1 to s_{10}) and remained in each space for 5 min, 3 times in total. Each reader was equipped with an antenna fixed in the appropriate direction during the test.

As shown in Table 3, the read rates for tags carried in backpacks were lower than those for tags carried in other ways (i.e., held in the hand, hung around the neck, in the front pocket, and in the back pocket). The read rates for tags carried in backpacks with no metal (Type *I*), low amounts of metal (Type *J*), middle amounts of metal (Type *K*), and high amounts of metal (Type *L*) were 98.0%, 97.3%, 92.7%, and 67.3%, respectively; statistical hypothesis tests were performed to determine whether the differences in read rates among the tags carried in backpacks with various amounts of metal were significant.

The read probability that each tag is read for tag-carrying type *i* (i.e., the read rates for Types *A* to *L* in Table 3) is denoted by p_i, and each tag type is assumed to have the same p_i in every test. Fifty tags were read in each test of type *i*, and Y_i has a binomial distribution with parameters 50 and an unknown p_i, represented by $Y_i \sim \text{Bin}[50, p_i]$. The variable n_i denotes the sample size of type *i* (i.e., the number of tests, $n_I = n_J = n_K = n_L = 3$), and Y_{ij} is the number of tags read in the *j*th test of type *i*. Therefore, Y_{I1}, Y_{I2}, and Y_{I3} yield a random sample of size n_i. The variable Y_{ij} can then be summed to represent the total number of tags read in tests of type *i*, and approximated to a normal random variable Z_i, defined in Eq. (4).

$$\sum Y_{ij} \sim Bin[50n_i, p_i] \approx Z_i \sim N[50n_i p_i, 50n_i p_i(1-p_i)] \tag{4}$$

The standard normal variable denoted by Z_{ij} can be used to test the null hypothesis H_0: $p_I = p_J$ (no difference in the mean read rate between Types *I* and *J*) against H_1: $p_I < p_J$ (a significant difference in the mean read rate between Types *I* and *J*). The hypothesis test results indicate that H_0 is rejected at a significance level α if the sample value of the test statistic Z_{ij} is lower than a critical value Z_α. Table 4 shows the hypothesis test results of the differences between the mean read rates of Types *I* and *J* ($\alpha = 0.01$). The results indicate that the test was expected to result in the acceptance of H_0 ($Z_{IJ} > Z_{0.01}$). In addition, there was no significant difference in mean read probabilities between tags exposed to no metal (Type *I*) and low amounts of metal (Type *J*). Table 5 shows the hypothesis test results of the differences between the mean read rates of Types *J* and *K* ($\alpha = 0.01$). Similarly, the results indicate that there was no significant difference in mean read probabilities between tags exposed to low metal (Type *J*) and middle amounts of metal (Type *K*). However, the hypothesis test results of the difference between the mean read rates of Types *K* and *L* ($\alpha = 0.01$) are presented in Table 6, suggesting that the test was expected to result in the rejection of H_0 ($Z_{KL} < Z_{0.01}$). In other words, there was a significant difference in mean read probabilities between middle amounts of metal (Type *K*) and high amounts of metal (Type *L*).

The Field Test I results indicated that the read rates of partially blocked readers were approximately 2% ~ 3% lower than those of readers in unobstructed spaces; the read rates of readers placed in crowded spaces were approximately 0.3% lower than those of readers in unobstructed spaces. These read rate decreases were determined to be within an acceptable range (<5%) for this study; thus, this device layout of gateways and readers (shown in Fig. 11) was used in an experiment designed to track RFID tags carried by participants. The Field Test II results indicate that read rates for tags carried by participants in backpacks were lower than those for tags carried in other ways, and the read rates of tags carried with no metal (Type *I*), low amounts of metal (Type *J*), and middle amounts of metal (Type *K*) did not

Table 4
Hypothesis test results for Types *I* and *J*.

Types	Metal effect	Mean read rate (%)	Z_{IJ}	$Z_{0.01}$
I	No	98.0	−0.382	>−2.326
J	Low	97.3	Accept H_0	

Table 5
Hypothesis test results for Types *J* and *K*.

Types	Metal effect	Mean read rate (%)	Z_{JK}	$Z_{0.01}$
J	Low	97.3	−1.854	>−2.326
K	Middle	92.7	Accept H_0	

Table 6
Hypothesis test results for Types *K* and *L*.

Types	Metal effect	Mean read rate (%)	Z_{KL}	$Z_{0.01}$
K	Middle	92.7	−5.485	<−2.326
L	High	67.3	Reject H_0	

significantly differ from the mean read rates. However, a significant difference was observed between the tags carried with middle amounts of metal (Type *K*) and tags carried with high amounts of metal (Type *L*). Therefore, during movement tracking RFID experiments, participants must be restricted to carrying a small amount of metal (less than 14-inch laptop).

6.3. Variables of function–space assignment

Eq. (1) is the objective function of function–space assignment, which includes two parts of weights. In this case, the two parts of weights were given the same importance by the decision maker ($W_1 = 0.5$, $W_2 = 0.5$), and the other variables of Eq. (1) were further explained as follows.

1. Suitability preference of function f_i assigned to space s_i ($P_{f_i s_i}$)

The spaces were divided into 3 groups, i.e., large (L: 90–135 m^2), medium (M: 45–80 m^2), and small (S: 15–20 m^2) spaces. Different functions require difference sizes of space. The library and seminar rooms prefer large spaces. The administration office and 2 laboratories prefer medium spaces. The 2 meeting rooms prefer small spaces. In addition, one of the classrooms prefers a medium space, and the rest of the two classrooms prefer large spaces. Table 7 provides the types of space size and the functions' preferred size.

The suitability preference for each possible pair of function–space assignment was given based on the following principles. A function requiring a large space can only be assigned to large space. Thus, the suitability preferences ($P_{f_i s_i}$) for the function assigned to large, medium, and small spaces were 1, 0, and 0, respectively. A function requiring a medium space can only be assigned to a large or medium (with less preference) space. Thus, $P_{f_i s_i}$ for the function assigned to large, medium, and small spaces was 0.5, 1, and 0, respectively. A function requiring a small space can be assigned to any space with different preferences. Thus, $P_{f_i s_i}$ for the function assigned to large, medium, and small spaces was 0.1, 0.5, and 1, respectively. The preference values between 0 and 1 were arbitrary depending on the decision maker, who, in this case, is the head of the department. The proposed model treated the zero preference as a constraint and never assigned a function to a space with $P_{f_i s_i} = 0$.

2. Distance between spaces s_i and s_j ($D_{s_i s_j}$)

The distance between spaces s_i and s_j was given based on the normalization of the sum of the actual geographical distance and weighted floor difference value of the two spaces. The weighted floor difference value was equivalent to 0 m if the two spaces are located on the same floor, such as s_5 and s_{10} in Fig. 9. The average user walking time for one-story staircase in this case is approximately 15 s, which is equivalent to 20-meter walking. Therefore, the weighted distance between two spaces located on two different consecutive floors, such as s_5 and s_4, is the sum of the horizontal distances plus 20 m. Similarly, the weighted value is 40 m and 60 m for the spaces situated 2 and 3 floors apart, respectively. Eq. (3) was used to normalize the weighted distance sum to ensure that the value falls between 0 and 1. Table 8 shows the normalized distances between the 10 spaces.

Table 8
Distance between space s_i and s_j.

$D_{s_i s_j}$	s_1	s_2	s_3	s_4	s_5	s_6	s_7	s_8	s_9	s_{10}
s_1	0.00	0.97	0.09	0.78	0.38	0.00	0.72	0.04	0.43	0.60
s_2	0.97	0.00	0.11	0.80	0.40	0.02	0.74	0.06	0.44	0.58
s_3	0.09	0.11	0.00	0.32	0.57	0.49	0.24	0.53	0.61	0.40
s_4	0.78	0.80	0.32	0.00	0.61	0.22	0.75	0.26	0.66	0.45
s_5	0.38	0.40	0.57	0.61	0.00	0.47	0.53	0.51	0.96	0.84
s_6	0.00	0.02	0.49	0.22	0.47	0.00	0.14	0.90	0.51	0.30
s_7	0.72	0.74	0.24	0.75	0.53	0.14	0.00	0.18	0.57	0.37
s_8	0.04	0.06	0.53	0.26	0.51	0.90	0.18	0.00	0.55	0.34
s_9	0.43	0.44	0.61	0.66	0.96	0.51	0.57	0.55	0.00	0.80
s_{10}	0.60	0.58	0.40	0.45	0.84	0.30	0.37	0.34	0.80	0.00

$$D_{s_i s_j} = \frac{D_x - D_{\min}}{D_{\max} - D_{\min}} \tag{3}$$

3. Movement relation of functions f_i and f_j ($R_{f_i f_j}$)

The movement relationship plays an important role in the optimization process. Table 9 shows the values of the interactive preference ($R_{f_i f_j}$), which was based on the movement analysis of the RFID tracking data. It signifies a usage pattern of an occupant between two functions. Basically, two functions with a large $R_{f_i f_j}$ should be located closer together to reduce the moving distance.

6.4. Function assignment results

The proposed model was installed on a Pentium 3.40 GHz PC with 512 MB RAM, with the parameters *epoch_max* and *era_max* set to 5 and 4, respectively. Table 10 shows the different function–space assignments suggested by the architect (row A_0), the proposed model (row R_1) versions, and their corresponding performances in terms of objective values. The R_1 version has a 14.80% higher objective value than the architect's version. The functions are also assigned to the space sizes most-preferred by the administrator (e.g., f_1 is assigned to the large spaces of s_6, f_5 is assigned to the small spaces of s_9). Additionally, the functions having larger $R_{f_i f_j}$ are also placed at least at the same floor (e.g., functions f_8 and f_9 and functions f_7 and f_9 are on floor 4).

The fmGA took approximately 16 s with the maximum generation equal to 20. As shown in Fig. 12, it actually required only 10 generations to converge to the optimal assignment (R_1). The performance is acceptable considering the problem has a combination size of 3,628,800 (=10!). In addition, with 10 generations of 448 populations, the number of solutions searched for by the proposed model was 4480 (=448 × 10), which was only 0.123% (=4480/3,628,800) of the search space.

Table 7
Space size and functions' preferred size.

Space	s_1	s_2	s_3	s_4	s_5	s_6	s_7	s_8	s_9	s_{10}
Size	M	M	L	M	S	L	M	L	S	L
Function	f_1	f_2	f_3	f_4	f_5	f_6	f_7	f_8	f_9	f_{10}
Preferred size	L	L	L	S	S	M	M	M	M	L
Description	Library	Classroom	Seminar room	Meeting room		Adm. office	Classroom	Laboratory		Classroom

Table 9
Movement relation of functions f_i and f_j.

$R_{f_i f_j}$	f_1	f_2	f_3	f_4	f_5	f_6	f_7	f_8	f_9	f_{10}
f_1		0.13	0.03				0.01		0.01	
f_2	0.16		0.02				0.11	0.01	0.02	0.06
f_3	0.01	0.04				0.02		0.04	0.06	
f_4										
f_5	0.01						0.02			0.02
f_6							0.08	0.07	0.01	
f_7		0.05			0.01	0.12	0.00		0.38	0.02
f_8	0.01		0.05	0.02		0.04	0.04		0.72	
f_9	0.01	0.01	0.01			0.03	0.09	0.75	0.00	
f_{10}			0.03		0.05	0.02	0.05		0.02	

6.5. Non-BBs vs. BBs

The proposed model, following Goldberg's suggestion [57], incorporated building-block filtering in its fmGA problem-solving process to generate enough copies of the good building blocks so more copies would remain for subsequent processing. To improve the efficiency, we removed the building-block filtering step from the model, in particular, Step 3 in the problem-solving process of Fig. 5. Thus, the non-BBs model has no filtering step, which consists of building-block selection and random gene deletion.

We conducted another experiment to compare the performance of the fmGA with and without building-block filtering (BBs vs. non-BBs) using 3 function assignment scenarios. Scenario I is the actual case described in the previous sections. Scenarios II and III are expanded from the first one to 20-story and 40-story buildings with 50 functions and 100 functions, respectively.

For building block selection, we selected 2, 10, and 20 pairs of functions with the highest movement relation values ($R_{f_i f_j}$) out of the C_2^{10}, C_2^{50}, and C_2^{100} combinations as the BBs for the 4-, 20-, and 40-story buildings, respectively. For example, for the 4-story building, (f_9 and f_8) and (f_7 and f_9) are the pairs with the highest $R_{f_i f_j}$ s, namely 0.75 and 0.38, respectively. We limited the search space by imposing two additional constraining rules. First, the chromosomes in one era were only retained if the two pairs of functions were assigned to neighboring spaces (with distance value $D_{s_i s_j} \geq 0.8$). Second, the random gene deletion operation, which randomly replaced genes for each of the lower halves of the populations in each era with the competitive template, should not replace the BBs.

Tables 11, 12 and 13 compare the performances between the fmGA with and without BBs in Columns (a), (b), and (c) for scenarios I, II, and III, respectively. For the 4-story building with 10 functions, there were no significant differences in terms of objective values. The converging generations for the BBs were decreased by 23.1% and 13.3%, but with 23.1% and 15.4% more total running time compared to the Non-BBs with 20 and 40 maximum generations, respectively. For the 20-story building with 50 functions, the BBs resulted in 7.8% and 5.8% higher objective values, and 17.3% and 2.9% less converging generations but with 452.6% and 412.1% more total running time for 800 and 1000 maximum generations, respectively. Similarly, for the 40-story building with 100 functions, the BBs resulted in 19.2% and 19.5% higher objective values, and 1.5% and 19.5% less converging generations but with 435.3% and 423.5% more total running time for 1600 and 1800 maximum generations, respectively.

Table 10
Result of function–space assignment.

Result	Function–space assignment										Objective value	
	s_1	s_2	s_3	s_4	s_5	s_6	s_7	s_8	s_9	s_{10}	Value	Improvement
A_0	f_8	f_9	f_3	f_7	f_5	f_2	f_{10}	f_1	f_4	f_6	1.1047	$(A_0 - A_0)/A_0$ 0.00%
R_1	f_8	f_9	f_{10}	f_7	f_4	f_1	f_6	f_2	f_5	f_3	1.2682	$(R_1 - A_0)/A_0$ 14.80%

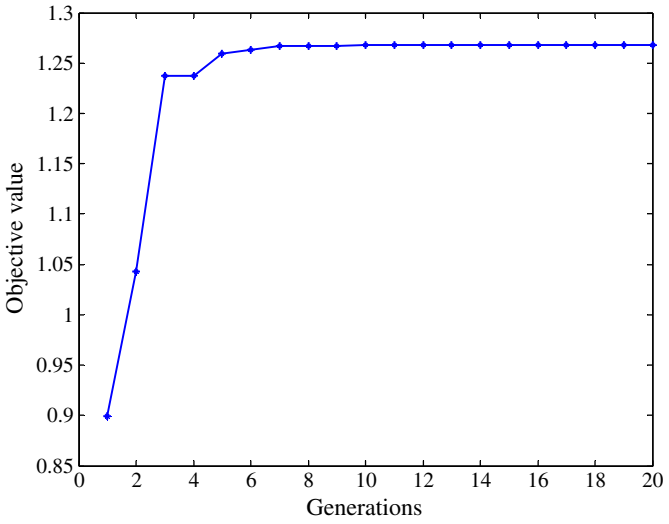

Fig. 12. Objective value of result R_1.

To further compare the required additional running time for non-BBs and BBs when the problem complexity increased, we repeated the 3 scenarios with the maximum generations fixed at 1000. Fig. 13 compares the required running times for non-BBs and BBs in scenarios with complexities of 50 to 250 functions.

Based on the experiment, the improvement in the objective value increased as the problem became more complicated (from 0.0% for the 4-story building to a 19.5% improvement for the 40-story building). The converging generations required for the BBs were always less than the non-BBs but appeared to be random without an obvious tendency. The total running time for the BBs was always more than for non-BBs. In addition, the proportions of additional time required due to the increased maximum generations were about the same for both non-BBs and BBs. For example, in Scenario I, the running times were approximately double the original running times when the maximum generation increased from 20 to 40 for both non-BBs and BBs. The increased proportion relationship also remains the same for Scenarios II and III. However, from Fig. 13, the benefit of time savings soon became obvious once the functions were greater than 100. Thus, for an assignment problem with less than 100 functions, we suggest the use of BBs. For a problem with greater than 100 functions, users need to consider the tradeoff between efficiency and solution quality because the BBs did find better assignments but with a significant cost in running time.

7. Conclusion

Assigning appropriate functions to building spaces is one of the most important factors in determining the use performance of a building. However, in architectural practice, architects and building owners renovate buildings based on their personal subjective perceptions of how occupants use the building instead of systematically analyzing their use behaviors. This research proposed a function–space assignment optimization model based on the occupants' movement data that was tracked using RFID technology. The model consists of 3 modules, namely movement tracking and positioning, occupants' movement analysis, and function–space assignment optimization. The model has contributed to the following several aspects: First, the movement tracking and positioning module is adopted to track the occupants' movement data in a building. Second, the occupants' movement analysis module is used to mine occupants' movement pattern and calculate the relation values between functions. Third, the function–space assignment module is employed to identify the optimal result of function assignment based on the derived relation values and the acceptable size for each space.

Table 11
Comparison of performance between Non-BBs and BBs in scenario I.

Scenario I (4-story building with 10 functions)

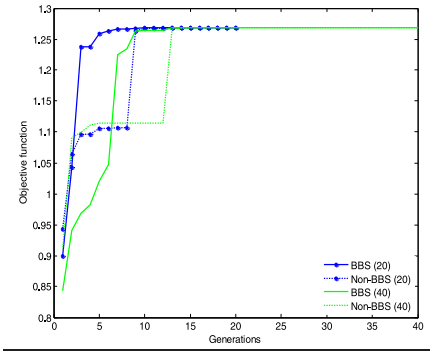

Max. generations	Performance	(a) Non-BBs	(b) BBs	(c) Difference [(b) − (a)]/[(a)]
20	Objective value	1.2681	1.2681	0.0%
	Converging generation	13	10	−23.1%
	Total running time (s)	13	16	23.1%
40	Objective value	1.2681	1.2681	0.0%
	Converging generation	15	13	−13.3%
	Total running time (s)	26	30	15.4%

Table 12
Comparison of performance between Non-BBs and BBs in scenario II.

Scenario II (20-story building with 50 functions)

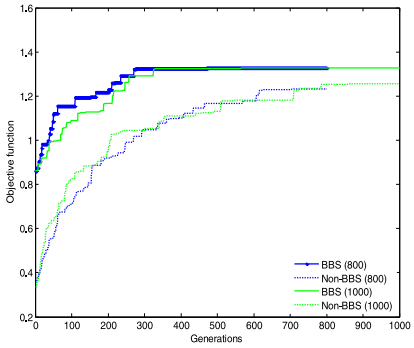

Max. generations	Performance	(a) Non-BBs	(b) BBs	(c) Difference [(b) − (a)]/[(a)]
800	Objective value	1.2312	1.3268	7.8%
	Converging generation	717	593	−17.3%
	Total running time (s)	371	2050	452.6%
1000	Objective value	1.2546	1.3274	5.8%
	Converging generation	953	925	2.9%
	Total running time (s)	463	2371	412.1%

In addition, an experiment with a real case also showed that the model can find better assignments than an architect showing a 14.8% higher objective value. The second experiment compares the performances of the model with and without the building-block filtering (BBs) mechanism. When the problem changes from simple to complex, we found that assignments with BBs are always equal or better than those with non-BBs showing an increase as high as 19.5% in the objective value; however, the running time increase as much as 4.35 times. With the maximum generation fixed at 1000, the difference in running time between the two models became obvious for assignments with greater than 100 functions.

Future research may include the following directions. First, the proposed model is demonstrated specifically for application of RFID tracking technology to the optimization of function–space assignment in an educational building, but it can be modified to apply to other similar function–space assignment problems for remodeling buildings, such as administration buildings, office buildings, general hospitals, museums, as well as membership wholesaler stores. Second, there are still several objectives that the proposed model did not address but are still considered significant in practice. Further research can extend the present objective function, such as thermal, visual, acoustics comfort, energy saving, cost, or safety perspectives, to gain a more comprehensive assignment.

Table 13
Comparison of performance between Non-BBs and BBs in scenario III.

Scenario III (40-story building with 100 functions)

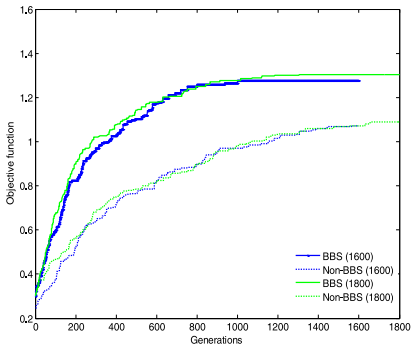

Max. generations	Performance	(a) Non-BBs	(b) BBs	(c) Difference [(b) − (a)]/[(a)]
1600	Objective value	1.0713	1.2770	19.2%
	Converging generation	1565	1541	−1.5%
	Total running time (s)	2252	12,054	435.3%
1800	Objective value	1.0896	1.3023	19.5%
	Converging generation	1729	1392	−19.5%
	Total running time (s)	2592	13,568	423.5%

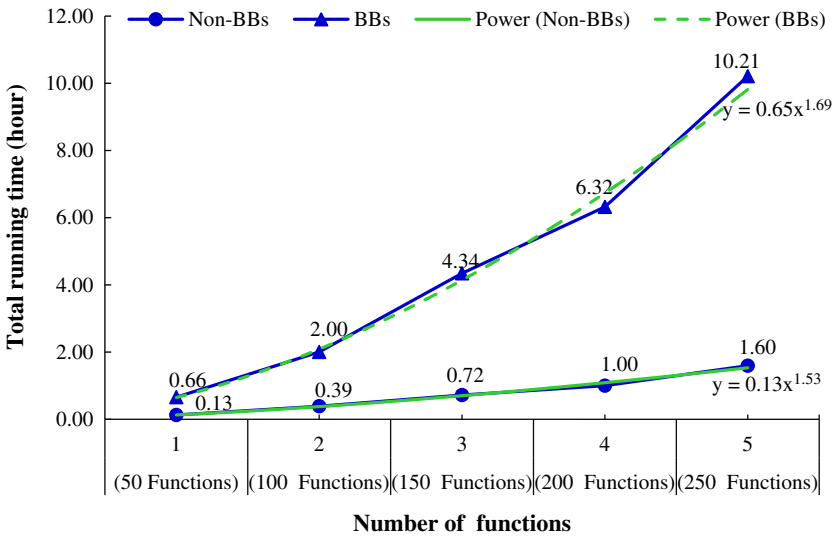

Fig. 13. Total running time in 1000 generations for the Non-BBs and BBs.

The experimental results indicate the usability of the proposed model, exhibiting a 14.8% improvement in objective value compared with the architect's version. It may be argued that, because of the high setup cost involved, acquiring the numerous RFID readers and tags the model requires is not economically beneficial for an educational facility. However, in the commercial sector, businesses such as membership wholesale stores may have an incentive to apply the model, for example, to optimize product arrangement and enable customers to find products easily. The model could also become more economically feasible by reducing the cost of collecting data. The price of RFID readers and tags is decreasing, and simulation software can also be used to simulate, instead of track, the movement of participants. We are currently extending the proposed system to include an activity simulation module that provides an alternative method for users to collect movement data.

Acknowledgments

This work was partially supported by the National Science Council grants (NSC 99-2221-E-009-133-MY3). Their support is greatly appreciated.

References

[1] Y.E. Kalay, Architecture's New Media: Principles, Theories, and Methods of Computer-aided Design, MIT Press, Cambridge, 2004.
[2] R. Choudhary, A. Malkawi, P.Y. Papalambros, Analytic target cascading in simulation-based building design, Autom. Constr. 14 (2005) 551–568.
[3] X. Ning, K.C. Lam, M.C. Lam, A decision-making system for construction site layout planning, Autom. Constr. 20 (2011) 459–473.
[4] F. Sadeghpour, O. Moselhi, S. Alkass, A CAD-based model for site planning, Autom. Constr. 13 (2004) 701–715.
[5] S.S.Y. Wong, K.C.C. Chan, EvoArch: an evolutionary algorithm for architectural layout design, Comput. Aided Des. 41 (2009) 649–667.
[6] R.S. Liggett, W.J. Mitchell, Optimal space planning in practice, Comput. Aided Des. 13 (5) (1981) 277–288.
[7] T.C. Koopmans, M. Beckman, Assignment problems and the location of economic activities, Econometrica 25 (1) (1975) 53–76.
[8] I.C. Yeh, Architectural layout optimization using annealed neural network, Autom. Constr. 15 (2006) 531–539.
[9] R.E. Burkard, Quadratic assignment problems, Eur. J. Oper. Res. 15 (1984) 283–289.
[10] P.M. Hahn, J. Jrarup, A hospital facility layout problem finally solved, J. Intell. Manuf. 15 (55/6) (2000) 1–11.
[11] R. Lee, J.M. Moore, CORELAP-computerized relationship layout planning, J. Ind. Eng. Comput. 18 (1967) 195–200.
[12] J.M. Seehof, W.O. Evans, Automated layout design program, J. Ind. Eng. Comput. 18 (1967) 690–695.
[13] J.A. Tompkins, J.R. Reed, An applied model for the facilities design problem, Int. J. Prod. Res. 14 (1976) 583–595.
[14] M.M.D. Hassan, G.L. Hogg, D.R. Smith, SHAPE: a construction algorithm for area placement evaluation, Int. J. Prod. Res. 24 (5) (1986) 1283–1295.
[15] G.C. Armour, E.S. Buffa, A heuristic algorithm and simulation approach to relative allocation of facilities, Manag. Sci. 9 (2) (1963) 294–300.
[16] T.M. Khalil, Facilities relative allocation technique (FRAT), Int. J. Prod. Res. 11 (2) (1973) 183–194.
[17] Z. Drezner, A heuristic procedure for the layout of a large number of facilities, Int. J. Manag. Sci. 33 (7) (1987) 907–915.
[18] E.M. Loiola, N.M.M.D. Abreu, P.O. Boaventura-Netto, P. Hahn, T. Querido, A survey for the quadratic assignment problem, Eur. J. Oper. Res. 176 (2007) 657–690.
[19] M. Solimanpur, P. Vrat, R. Shankar, An ant algorithm for the single row layout problem in flexible manufacturing systems, Comput. Oper. Res. 32 (3) (2005) 583–598.
[20] L.Y. Liang, W.C. Chao, The strategies of tabu search technique for facility layout optimization, Autom. Constr. 17 (2008) 657–669.
[21] S.O. Cheung, T.K. Tong, C.M. Tam, Site pre-cast yard layout arrangement through genetic algorithms, Autom. Constr. 11 (2002) 35–46.
[22] H. Jang, S. Lee, S. Choi, Optimization of floor-level construction material layout using Genetic Algorithms, Autom. Constr. 16 (2007) 531–545.
[23] J.H. Holland, Adaptation in Natural and Artificial System, Univerity of Michigan, Ann Arbor, 1975.
[24] H.K. Juan, J.H. Kim, K. Roper, D. Castro-Lacouture, GA-based decision support system for housing condition assessment and refurbishment strategies, Autom. Constr. 18 (2009) 394–401.
[25] H. Li, P.E.D. Love, Genetic search for solving construction site-level unequal-area facility layout problems, Autom. Constr. 9 (2000) 217–226.
[26] D.E. Goldberg, B. Korb, K. Deb, Messy genetic algorithms: motivation, analysis, and first results, Compl. Syst. 3 (5) (1989) 493–530.
[27] D.E. Goldberg, K. Deb, H. Kaegupta, G. Harik, Rapid, accurate optimization of difficult problems using fast messy genetic algorithms, Proceedings of the Fifth International Conference on Genetic Algorithms, 1993, pp. 56–64.
[28] D. Halhal, G.A. Walters, D.A. Savic, D. Ouazar, Scheduling of water distribution system rehabilitation using structured messy genetic algorithms, Evol. Comput. 7 (3) (1999) 311–329.
[29] C.W. Feng, H.T. Wu, Integrating fmGA and CYCLONE to optimize the schedule of dispatching RMC trucks, Autom. Constr. 15 (2) (2006) 186–199.
[30] F. Hoffmann, G. Pfister, Learning of a fuzzy control rule base using messy genetic algorithms, in: F. Herrera (Ed.), Genetic Algorithms and Soft Computing, Physica-Verlag, Heidelberg, 1996, pp. 279–305.
[31] C.K. Mohan, A messy genetic algorithms for clustering, in: C.H. Dagli, L.I. Burke, B.R. Feranadez, J. Ghosh (Eds.), Intelligent Engineering Systems Through Artificial Neural Networks, ASME Press, New York, 1993, pp. 831–836.
[32] P.L. Lanzi, Extending the representation of classifier conditions Part I: From binary to messy coding, Proc. Genet. Evol. Comput. Conf. 1 (1999) 337–344.
[33] P.L. Lanzi, A. Perrucci, Extending the representation of classifier conditions Part ΠΙ: From messy coding to S-expressions, Proc. Genet. Evol. Comput. Conf. 1 (1999) 345–352.
[34] A.N. Skurikhin, A.J. Surkan, Messy genetic algorithm learns a classifier to design multiplexers, Proceedings of 1996 IEEE international conference on, evolutionary computation, 1996, pp. 100–103.
[35] M.Y. Cheng, Y.W. Wu, C.F. Wu, Project success prediction using an evolutionary support vector machine inference model, Autom. Constr. 19 (3) (2010) 619–629.
[36] M. Paciga, H. Lutfiyya, Herecast: an open infrastructure for locationbased services using WiFi, Wireless and mobile computing, networking and communications (WiMobapos), 4, IEEE IC, 2005, pp. 21–28.
[37] R. Want, A. Hopper, V. Falcao, J. Gibbons, The active badge location system, ACM Trans. Inf. Syst. 40 (1) (1992) 91–102.
[38] L. Ran, S. Helal, S. Moore, Drishti: an integrated indoor/outdoor blind navigation system and service, Proceedings of the second IEEE annual conference on pervasive computing and communications, 2004, pp. 23–30.

[39] T. Dowad, PAWS: personal action wireless sensor, Pers. Ubiquit. Comput. 10 (2–3) (2006) 173–176.
[40] N. Li, B. Becerik-Gerber, Performance-based evaluation of RFID-based indoor location sensing solutions for the built environment, Adv. Eng. Inform. 25 (2011) 535–546.
[41] R. Tesoriero, R. Tebar, J.A. Gallud, M.D. Lozano, V.M.R. Penichet, Improving location awareness in indoor spaces using RFID technology, Expert Syst. Appl. 37 (2010) 894–898.
[42] G. Saeed, A. Brown, M. Knight, M. Winchester, Delivery of pedestrian real-time location and routing information to mobile architectural guide, Autom. Constr. 19 (2010) 502–517.
[43] J. Song, C.T. Haas, C. Caldas, E. Ergen, B. Akinci, Automating the task of tracking the delivery and receipt of fabricated pipe spools in industrial projects, Autom. Constr. 15 (2006) 166–177.
[44] M.N. Lionel, Y.H. Liu, Y.C. Lau, A.P. Patil, LANDMARC: indoor location sensing using active RFID, Wirel. Netw 10 (6) (2004) 701–710.
[45] J.F. McCarthy, D.H. Nguyen, A.M. Rashid, S. Soroczak, Proactive displays and the experience UbiComp Project, Proceedings of the Fifth International Conference on Ubiquitous Computing, 2003, pp. 78–81.
[46] E.J. Jaselskis, M.R. Anderson, C.T. Jahren, Radio-frequency identification applications in construction industry, J. Constr. Eng. Manag. 121 (2) (1995) 189–196.
[47] W.S. Jang, M.J. Skibniewski, Embedded system for construction asset tracking combining radio and ultrasound signals, J. Comput. Civ. Eng. 23 (4) (2009) 221–229.
[48] P.M. Goodrum, M.A. McLaren, A. Durfee, The application of active radio frequency identification technology for tool tracking on construction job sites, Autom. Constr. 15 (3) (2006) 292–302.
[49] K. Dziadak, B. Kumar, J. Sommerville, Model for the 3D location of buried assets based on RFID technology, J. Comput. Civ. Eng. 23 (3) (2009) 148–159.
[50] K. Domdouzis, B. Kumar, C. Anumba, Radio-Frequency Identification (RFID) applications: a brief introduction, Adv. Eng. Inform. 21 (4) (2007) 350–355.
[51] C.T. Tzeng, T.C. Chiang, C.M. Chiang, C.M. Lai, Combination of radio frequency identification (RFID) and field verification tests of interior decorating materials, Autom. Constr. 18 (2008) 16–23.
[52] L.C. Wang, Enhancing construction quality inspection and management using RFID technology, Autom. Constr. 17 (2008) 467–479.
[53] S. Chin, S. Yoon, C. Choi, C. Cho, RFID + 4D CAD for progress management of structural steel works in high-rise buildings, J. Comput. Civ. Eng. 22 (2) (2008) 74–89.
[54] S.Y.L. Yin, H.P. Tserng, J.C. Wang, S.C. Tsai, Developing a precast production management system using RFID technology, Autom. Constr. 18 (2009) 677–691.
[55] N. Li, S. Li, B. Becerik-Gerber, G. Calis, Deployment strategies and performance evaluation of a virtual-tag-enabled indoor location sensing approach, J. Comput. Civ. Eng. 26 (5) (2012) 574–583.
[56] J.R. Jo, J.S. Gero, Space layout planning using an evolutionary approach, Artif. Intell. Eng. 12 (3) (1998) 149–162.
[57] D.E. Goldberg, The Design of Innovation: Lessons From and for Competent Genetic Algorithms, Kluwer Academic, Boston, 2002.
[58] D.E. Goldberg, K. Deb, B. Korb, Don't worry, be messy, Proceedings of the Fourth International Conference on Genetic Algorithms, 1991, pp. 24–30, La Jolla, CA.